ACSNANO

www.acsnano.org

ARTICLE

Direct Observation of the Release of Nanoplastics from Commercially Recycled Plastics with Correlative Raman Imaging and Scanning Electron Microscopy

Wen Zhang,[†] Zhiqiang Dong,[†] Ling Zhu, Yuanzhang Hou, and Yuping Qiu*

Cite This: https://dx.doi.org/10.1021/acsnano.0c02878

Read Online

ACCESS | Metrics & More | Article Recommendations | Supporting Information

ABSTRACT: Nanoplastics (NPs), mainly originated from weathering of microplastics, are ubiquitous throughout the world. However, the environmentally released NPs are still under debate due to the lack of direct proof for the chemical identification of individual nanoparticles. Here, we show an observational evidence of release of heterogeneous NPs from recycled PVC powders (RPP) using a nondestructive analytical method, namely, correlative Raman imaging and scanning electron (RISE) microscopy. The technology achieves direct chemical identification of individual nanoparticles on RPP surface that are as small as 360 nm including nano-PVC and nano-$CaCO_3$ in complexes with pigments. After washing and filtering through a 1 μm poly(ether sulfone) filter, we clearly distinguish nano-PVC from the other components in an air-dried filtrate. Furthermore, the automated 2D mapping of RISE enables the acquisition of the 2D chemical information on a selected area (*e.g.*, 5 μm × 5 μm) and the display of the different components of nanoparticle aggregates without colloidal separation. Our findings give direct evidence and detailed insights in the potential release of nanoplastics from the recycled plastic products. The RISE method will help us intuitively understand the origin, occurrence, and fate of NPs in the environment.

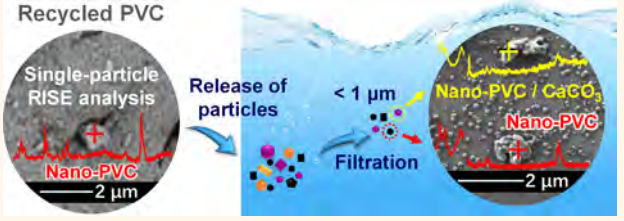

KEYWORDS: *nanoplastics, microplastics, polyvinyl chloride, Raman imaging and scanning electron (RISE) microscopy, single-nanoparticle analysis, direct chemical identification, environmental release*

Recent research has observed nanoplastics (NPs, less than 1 μm in one dimension[1,2]) in marine environments.[3] NPs are deemed to arise indirectly from the fragmentation of large plastic debris in the ocean[4,5] and directly from daily commodities, such as cosmetic products and drug carriers.[6−8] However, direct observational evidence that supports these hypotheses are lacking. NP-like components can be obtained from light degradation[9] and mechanical breakdown[10] of polystyrene plastic materials, but chemical information on monogranular NPs remains unknown. Hernandez et al.[7] claimed that 24−52 nm ultrafine polystyrene particles can be separated from microbead-containing commercial facial scrubs by sequential filtration. In other cases, secondary NPs might be produced from biodegradable polyhydroxybutyrate microplastics (MPs),[11] and a plastic teabag can release billions of NPs into a single cup.[12] Nevertheless, these isolated nanomaterials are identified by analyzing the thin powder film of particle aggregates from the drying suspension primarily by using attenuated total reflectance Fourier transform infrared (ATR-FTIR) spectroscopy.[11,12]

Innovative techniques have been developed in recent years for the direct analysis of the chemical compositions of discernible NP particles in environmental samples. For example, hyperspectral imaging (HSI), which combines spectral image information from 200 to 2500 nm and spatial image information,[13,14] enables the determination and visualization of MPs and NPs in complex biological or environmental matrices.[15] The chemicals of each pixel is identified by using spectral information obtained through a mathematical model.[16] However, the HSI technology is unsuitable for

Received: April 5, 2020
Accepted: May 22, 2020
Published: May 22, 2020

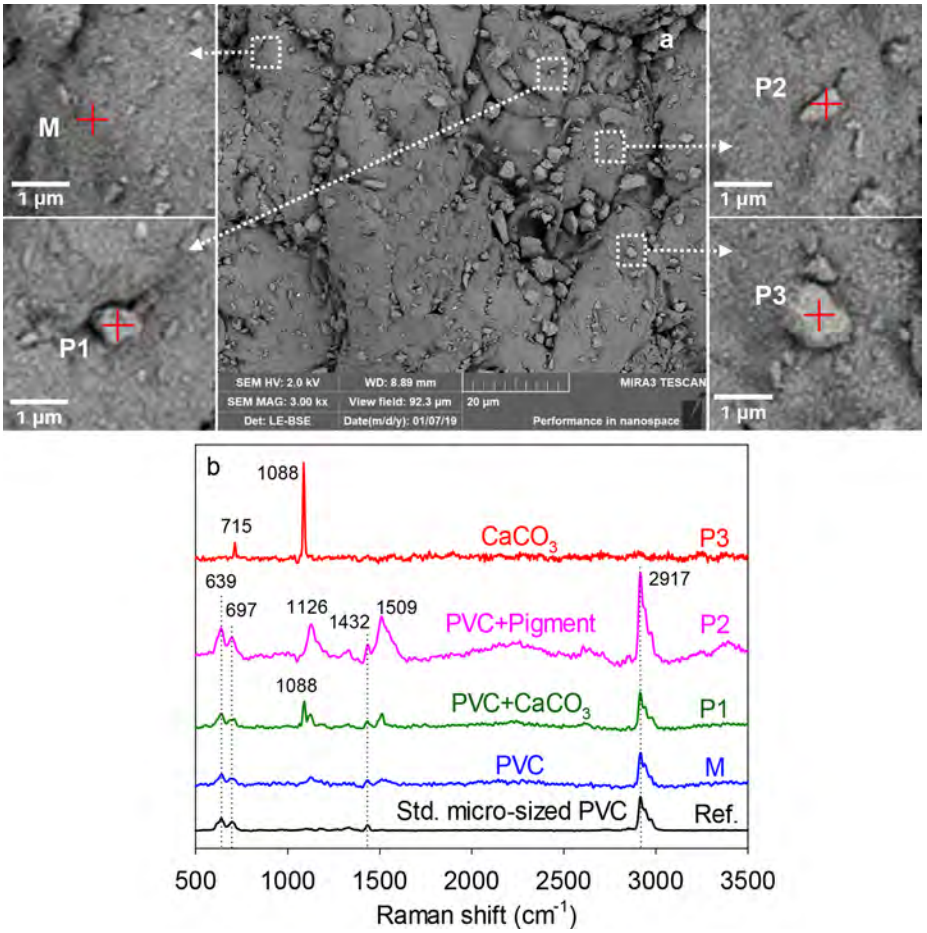

Figure 1. Scanning electron microscopy (SEM) images and Raman spectroscopy of nanoparticles on the suface of recycled PVC powders (RPP). (a) SEM images of the matrix (M) of recycled PVC powders (RPP) and the selected nanoparticles (P1, P2, and P3) on RPP surface. (b) Raman spectra (532 nm laser) recorded with the confocal Raman-in-SEM system. Peaks for standard PVC: 639, 697, 1178, 1333, 1432, and 2917 cm^{-1}.[27] Peaks for standard $CaCO_3$: 715 and 1088 cm^{-1} (Supplementary Figure 3). Peaks for pigments: 1126 and 1509 cm^{-1} (Supplementary Figure 2b).[28−30]

determining NPs in homogeneous plastic background matrices because HSI imaging is primarily used for visualizing spatial heterogeneities.[17]

Raman spectroscopy is a nondestructive analysis technique for the characterization of plastic chemical structures on the basis of detected vibrations that modify the polarizability of a polymer molecule.[18,19] Recently, the integration of Raman imaging and scanning electron microscopy (SEM) was realized in one instrument, namely, the confocal Raman-in-SEM system.[20−22] This technique enables the acquisition of morphological images at nanometer resolutions and the chemical compositions of nanopolymer particles.[20−22]

As a high-strength thermoplastic polymer, polyvinyl chloride (PVC) is extensively used in pipes, buildings, and structures.[23,24] The recycling of primary plastic wastes into recycled plastics is an important part of global efforts for the reduction of plastics in the waste stream.[25] Recycled PVC is often pulverized in fine powder for subsequent plastic injection, molding, and combination with other ingredients.[26] The grinding process of recycled PVC powder can generate nanosized PVC particles.

Herein, we applied correlative RISE microscopy for the direct identification and morphological characterization of the possible nanoparticles on the surface of recycled commodity PVC powder. Furthermore, nanoparticles washed off from the powder surfaces were individually identified through RISE method and used in determining whether nanosized PVC can be released by washing with distilled water. By performing Raman single-spot analysis on the NPs from the shedding of PVC powder, we were able to observe directly the potential release of NPs from commercially available recycled plastic materials.

RESULTS AND DISCUSSION

Direct Chemical Identification of the Observed Nanoparticles on RPP Surface. Fourier transform infrared (FTIR) microscopy results preliminarily demonstrated that the recycled PVC powder (RPP) basically consists of PVC and calcium carbonate ($CaCO_3$) components (Supplementary Figure 1a). The detailed FTIR analysis is presented in the Supporting Information (Supplementary Text 1 and Supplementary Figure 1b). RISE was innovatively used in observing ultrafine particles (0.1−1 μm) with different irregular shapes on the RPP surface and directly identifying the chemical and structural characteristics of these nanoparticles (Figure 1a). Prior to identification, the Raman spectrum of a standard microsized PVC was obtained by the Raman-in-SEM system (Figure 1b) and used as a reference. The representative Raman spectral features of the standard microsized PVC were characteristic adsorption peaks at 639 and 697 cm^{-1}, which

https://dx.doi.org/10.1021/acsnano.0c02878
ACS Nano XXXX, XXX, XXX−XXX

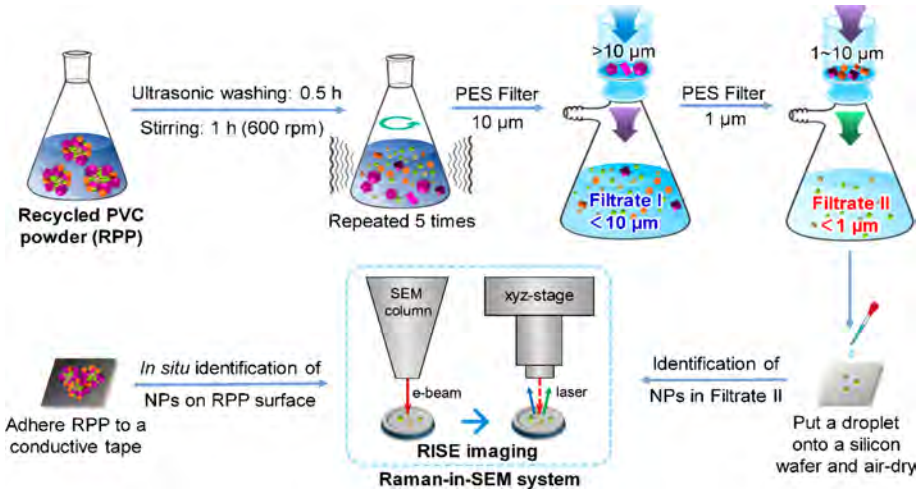

Figure 2. Procedure of the experiment. The nanoparticles on the suface of recycled PVC powders (RPP) was directly observed and identified via RISE technique. The RPP was first imaged with the SEM microscope function to obtain the nanoparticle morphology. Subsequently, the sample was automatically transferred and repositioned for confocal Raman imaging to measure the Raman spectrum of the selected nanoparticles. The released nanoparticles were obtained via the stirring−ultrasonic washing approaches and two filtration steps (10 μm, 1 μm). The filtrate II was drop-casted on silicon wafer and subsequently air-dried for the conduct of RISE analysis.

are assigned to the C−Cl stretching vibration in the PVC polymer.[27] In addition, the adsorption peaks at 1178, 1432, and 2917 cm^{-1} correspond to the C−H rocking vibration, C−H bending vibration, and C−H stretching vibration, respectively.[27] These results were similar to the Raman spectrum of RPP matrix, indicating C−Cl stretching vibration (639 and 697 cm^{-1}), C−H bending vibration (1432 cm^{-1}), and C−H stretching vibration (2917 cm^{-1}; Figure 1b).

The RISE imaging is efficient for the direct characterization of nanoparticles on the RPP surface. The selected nanoparticles (P1, P2, P3, and P4) were identified by confocal Raman-in-SEM (λ_{ex} = 532 nm; Figure 1b and Supplementary Figure 2). P1 and P2 present the typical characteristic peaks of PVC at 639, 697, 1432, and 2917 cm^{-1} (Figure 1b), indicating that the PVC ingredient dominates these nanoparticles. The characteristic peak of $CaCO_3$ at approximately 1088 cm^{-1} was observed in P1, demonstrating that P1 might be the mixture of PVC and $CaCO_3$ (Figure 1b). In addition, P2 presented the adsorption peaks at approximately 1126 and 1509 cm^{-1}, corresponding to the C−C and C═C of polyene chain structures, respectively.[28] These structures can be attributed to the characteristic peaks of pigments, comprising a series of additives frequently used in polymer blends.[29,30] However, P3 was confirmed as a $CaCO_3$ particle according to the typical absorption peaks at 715 and 1088 cm^{-1}, respectively (Figure 1b), which was perfectly matched with those of standard $CaCO_3$ (Supplementary Figure 3). Furthermore, P4 exhibited the predominant peaks located at 1126 and 1509 cm^{-1} (Supplementary Figure 2b), suggesting that the P4 particle is composed of pure polyene pigment.[29,30]

Characteristics of the Released Nanoparticles from RPP. These observed nanoparticles were isolated from the RPP surface in ultrapure water by stirring and ultrasonic washing (Figure 2). The SEM image demonstrated that the tiny particles on the surface of RPP nearly disappeared (Supplementary Figure 4). The total organic carbon (TOC) analyses revealed that the maximum TOC concentration in filtrate II remained constant at 9.69 ± 0.04 mg/L (Supplementary Table 1), implying that the quantitatively important release of organic matter is associated with nanoparticle colloids. Further calculation showed that approximately 0.15‰ (*w*/*w*) water-soluble and/or nanosized organic carbon substances could be washed off from RPP (Supplementary Table 1).

The filtrate II from RPP washing, which was passed through a 1 μm poly(ether sulfone) (PES) filter, was not stabilized due to the low ζ-potential (−16.93 ± 1.39 mV; Figure 2, Supplementary Table 1). The suspension probably consisted of different nanoparticles, PVC additives, and other organic substances.[31] The autocorrelation curve analysis demonstrated that the size of the released nanoparticles was concentrated at 300−1000 and 50−200 nm (Supplementary Figure 5). After air-drying, the morphology of nanoparticles in filtrate II was observed via SEM. The results indicated that they were highly polydisperse and had open structures (Figure 3a), which was similar to the fractal nature of aggregates, and no single parameter can be used to describe the particle population.[32]

Identification of the Released Nanoparticles and/or their Aggregates. Figure 3 and Supplementary Figure 6 show the SEM images of nanoparticles and/or their aggregates (S1−S5) from an air-dried droplet on a silicon wafer and their Raman spectrum (532 nm laser) recorded with RISE. The droplet was derived from filtrate II (Figure 2). These selected nanoparticles and/or their aggregates were analyzed by a Raman-in-SEM system. Prior to analyses, the standard nanosized PVC particles with different sizes (300−1920 nm) were targeted in SEM views (Supplementary Figure 7) and then measured by confocal Raman microspectroscopy. Results exhibited the typical Raman spectral information on 622 and 667 cm^{-1} corresponding to the C−Cl stretching vibration (Figure 3b), which has Raman characteristic absorption peaks similar to those of the S1 nanoparticle (Figure 3b). The ultrasonic washing process can release PVC-based NPs. RISE further discovered that S2 and S3 particles contain mixtures of PVC and $CaCO_3$, and the S4 particle was composed of PVC and pigment. The nano-$CaCO_3$-based S5 was observed (Supplementary Figure 6). The relatively weak peaks of C−Cl and C−H of S5 might be associated with the coating of the dissolved organic matter (*e.g.*, PVC macromolecule and additives leached from RPP) on $CaCO_3$.[31]

https://dx.doi.org/10.1021/acsnano.0c02878
ACS Nano XXXX, XXX, XXX−XXX

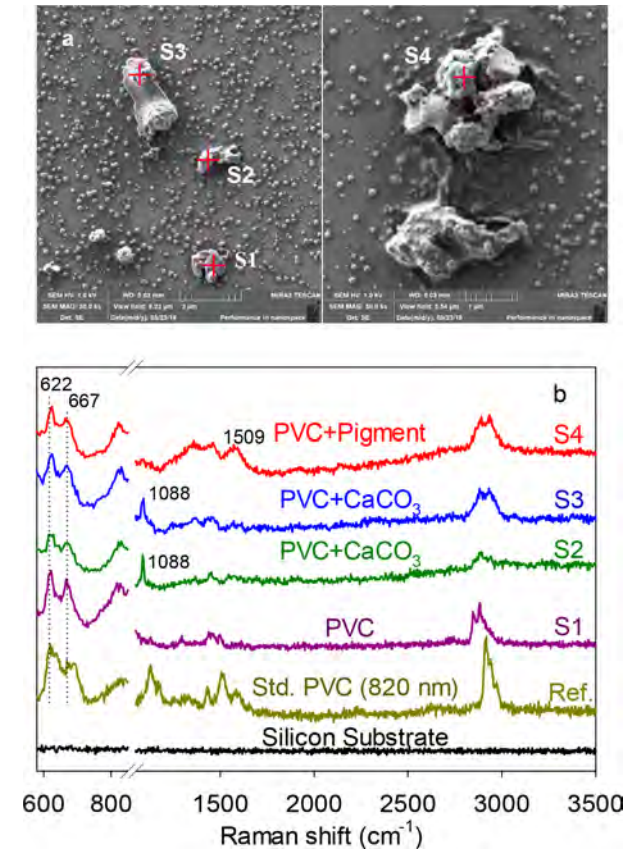

Figure 3. Scanning electron microscopy (SEM) images and corresponding Raman spectroscopy of nanoparticles released from the recycled PVC powders (RPP). (a) SEM images of nanoparticles and/or their aggregates (S1, S2, S3, and S4) from an air-dried droplet on a silicon wafer. (b) Raman spectrum (532 nm laser) recorded with confocal Raman-in-SEM system.

Supplementary Figure 5 indicates that the size of nanoparticles in filtrate II was less than 1000 nm. However, the nanoaggregates could be formed at a silicon substrate during air-drying prossess (Figure 4a). RISE provided the automatic mapping for discriminating the chemical composition of nanoaggregates in a selected area in silicon wafer, as described in Figure 4. This method made a precise description of the chemical information and two-dimension morphology of different components in aggregates according to the selected characteristic peaks of PVC (622 and 667 cm^{-1}), pigment (1509 cm^{-1}), and $CaCO_3$ (1088 cm^{-1}). The selected area of 5 μm × 5 μm was indicated with color markers (Figure 4a,b): The blue, red, and green colors represent the PVC, pigment, and $CaCO_3$, respectively (Figure 4c–e). Notably, the area of PVC correlated well with that of pigment, suggesting that PVC combined with the pigment. This phenomenon could be associated with the even dispersion of the pigment and plastic in the polymer blend by heating and melting during PVC production.[29] By contrast, the distribution of $CaCO_3$ was relatively centralized because $CaCO_3$ particles were directly added into the polymer matrix, making it difficult to achieve stable dispersion.[33]

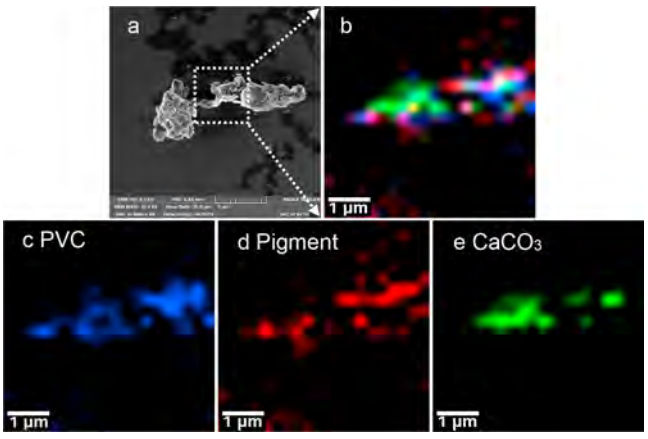

Figure 4. Raman spectral mapping of nanoparticles released from RPP. (a) Confocal Raman-scanning electron microscopy (SEM) image of a nanosized PVC/Pigment/$CaCO_3$ composite. (b) Color-coded Raman image overlaid on the SEM. (c) Corresponding blue area: PVC. (d) Corresponding red area: pigments. (e) Corresponding green area: $CaCO_3$.

Technical Advantages and Challenges of RISE Analysis. Direct chemical identification of individual nanoparticles is of technical challenge,[34,35] but it is the most convincing evidence for observing the release of nanomaterials. Although the possible release sources of environmental NPs have been widely studied, common analytical techniques including ATR-FTIR, micro-Raman, XPS, and GC–MS could not offer direct and visible evidence to identify the components of monoparticulate NP.[18,19] Recently, Gillibert et al.[36] introduced the Raman Tweezers technique, combined with Raman spectroscopy, to investigate individual NPs in an aquatic environment. However, the limitation of optical microscopy considerably restricted the quality of image of nanoparticles. At a diameter of less than 500 nm, the optical image only represents the laser spot size rather than the actual nanoparticle size due to the effect of optical diffraction.[36] RISE has a lower resolution (360 nm) than Raman Tweezers. Furthermore, RISE presented the identification of chemical compositions of nanoaggregates and their physical shapes. In this work, the released ingredients of commercial PVC, including nano-PVC and nano-$CaCO_3$ in complex with pigment were visually differentiated (Figure 1b), which has not been documented.[10,13]

The direct chemical identification of nanoparticles on the RPP surface suggests that recycled commodity plastics are a potential source of NPs. The RPP samples were derived from the pulverization of daily plastic wastes and planned as secondary raw materials partly instead of virgin polymers.[37] The mechanical recycling rate for plastic waste is approximately 30% in Europe.[38] The increasingly growing recycled plastics would significantly increase the release risk of NPs to the environment.

To explore the potential release of NPs, we obtained the leachate from RPP by stirring and ultrasonic washing (Figure 2). After washing with ultrapure water, the tiny particles on the RPP surface nearly disappeared (Supplementary Figure 4) and the TOC concentration in filtrate II was maintained at 9.69 ± 0.04 mg/L (Supplementary Table 1). Hence, environmental nanoparticles would be released from bulk plastics by water shear forces.[39] Sequentially, RISE was successfully applied for the identification of the observed nanoparticles. Both silicon and aluminum substrates were used for the RISE analyses of standard PVC nanoparticles with different sizes (Supplementary Figure 8). The disadvantage of a silicon substrate is that it brings strong background peaks located at 850–1050 cm^{-1}.

https://dx.doi.org/10.1021/acsnano.0c02878
ACS Nano XXXX, XXX, XXX–XXX

Nonetheless, these strong peaks do not overlap the characteristic peaks of PVC, $CaCO_3$, and pigment (Supplementary Figure 8a). Furthermore, the intensity of the Raman signal of these nanometer substances on a silicon wafer is much stronger than that on aluminum foil. Hence, the silicon wafer is preferred for the Raman analysis of standard PVC nanoparticles. Notably, a Raman redshift was observed, and the PVC characteristic peak intensity decreased with the decrease in particle size (Supplementary Figure 8a,b). As the PVC size decreased from 1450 to 300 nm, the position of C−Cl stretching vibration decreased from 635 to 621 cm^{-1} on the silicon substrate (Supplementary Figure 8a). When the size is less than 200 nm, the distinguishable Raman response signal can hardly be obtained.[36] The smaller the particle (especially less than 1 μm) the more significant the redshift (Supplementary Figure 8c). A similar phenomenon was observed in low-dimensional semiconductor nanocrystals, such as CdSe ZnO, CeO_2, and SnO_2.[40] The underlying mechanism behind the redshift of Raman peak for nanoparticles is presumably involved in the phonon confinement effect, surface stress, and structural defects.[40−42]

Due to the presence of size-dependent Raman effect, the Raman spectrum of 820 nm standard PVC nanosphere was selected as the reference in this study for the identification of the unknown nanoparticles because of its similar size to the size of the most observed nanoparticles. To eliminate the interference of Si signal, we cut off the Raman spectral range from 850 to 1050 cm^{-1} (Figure 3a,b). The good matching of characteristic peaks (622 and 667 cm^{-1} of the C−Cl stretching vibration) between standard PVC and the real PVC-contained nanoparticles in Figure 3b suggests that RISE could achieve the fixed-point analysis of monogranular NP. The measurement of Raman Tweezers requires NP concentration of 0.2% (w/w) for easy trapping and analysis, which was far higher than that in the nature aquatic environment.[36] Additionally, the TOC of leachate contributed by nanoparticle-contained dissolved organic matter in this work was only 9.69 ± 0.04 mg/L (Supplementary Table 1), which might be close to the real concentration of NPs in the environment. By contrast, RISE is the most effective technique for the identification of nanosized plastics on solid surfaces and in solutions.

In a natural aquatic environment, NPs tend to form heteroaggregates with numerous inorganic and organic particles.[2,43] The identification of NPs from environmental aggregates or matrices is challenging because of their tiny sizes and intricate interactions.[35] Currently techniques including size-based approaches, density-based approaches, and chemical separation for isolating microplastics from the environmental samples are not suitable to separate NPs.[35] Without complicated colloid separation, the Raman mapping could systematically offer 2D chemical information on a selected area to identify the components of nanoaggregates (Figure 4). Therefore, RISE is an efficient tool to obtain and chemically identify NP components in environmental matrices without a series of complicated separation operations.

CONCLUSIONS

In summary, RISE was successfully applied for the chemical analysis of NPs at the nanoscale. RISE demonstrated that RPP, a kind of commercially recycled plastic, is the potential release source of NPs. The morphological and chemical information on NPs could be concurrently obtained by analyzing a monogranular nanosubstance. The automatic mapping of RISE efficiently offered 2D chemical composition of the selected area to discriminate PVC from the other components in nanoaggregates without colloid separation. Our work achieved the direct observation and identification of individual NPs released from the surface of recycled commodity plastics, thus further elucidating the potential source of NPs in the environment.

MATERIALS AND METHODS

Materials. Recycled commodity plastics (PVC powder) were purchased from Yaxing Plastic Products Co. Ltd. (Dingzhou, Hebei Province, China); they were mechanically prepared from disused PVC tubes widely applied in daily life.[23,24] The PVC composition was confirmed by FTIR by using a Nicolet 5700 FTIR spectrometer. The average particle size of PVC powder (d_{50}) was 199 ± 20 μm (Supplementary Table 1), as determined by laser scattering particle size distribution analysis (LA-960, HORIBA, Ltd., Kyoto, Japan) (Supplementary Figure 9). The surface area of PVC powder was 88.26 m^2/kg (Supplementary Table 1) as determined via a multipoint BET (Brunauer, Emmett, and Teller) method by using N_2 adsorption at 77 K *via* a surface area analyzer (ASAP 2020, Micromeritics, Norcross, GA). The morphology of PVC was visualized via SEM (MAIA3 GMU, TESCAN, Brno, Czech Republic).

The standard microsized PVC with most of particle size in 60−200 μm (Supplementary Figure 10a) was obtained from Shanghai Aladdin Bio-Chem Technology Co., Ltd. (Shanghai, China). The standard nanosized PVC with most of particle size in 400−1000 nm (Supplementary Figure 10b) was purchased from Shanghai GuanBu Electromechanical Technology Co., Ltd. (Shanghai, China).

Direct Observation and Identification of Nanoparticles on RPP Surface. To observe and identify the possible nanoparticles on PVC powder, we used a novel correlative RISE technique, which combines SEM and confocal Raman microscopy within the Raman-in-SEM system with a high spatial resolution down to 360 nm (MAIA3 GMU, TESCAN, Brno, Czech Republic). The electron acceleration voltage in SEM was set to 2 kV. The Raman spectroscopy operated at a 532 nm laser excitation wavelength with 5 mV laser energy, which is the optimized power and does not damage the PVC structure. The PVC powder was first imaged with the SEM microscope function to obtain the nanoparticle morphology. Subsequently, the sample was automatically transferred and repositioned for confocal Raman imaging within the vacuum chamber of the electron microscope to measure the Raman spectrum of nanoparticles. As an example of standard microsized PVC, RISE analysis can also achieve good image location and matching accuracy between SEM and Raman (Supplementary Figure 11).

Release of Nanoparticles from RPP by Washing. Simple physical approaches, including stirring and ultrasonic washing, were applied for the removal of NPs from the surface of PVC powders (Figure 2). In brief, 10 g of PVC powder was placed in a 250 mL Erlenmeyer flask with 150 mL of Milli-Q ultrapure water. After sealing to avoid water evaporation, the flask was stirred at 600 rpm for 1 h under vigorous magnetic stirring and then sonicated in an ultrasonic cleaner (SK3200HP, KUDOS, China) for 30 min. The stirring and ultrasonic processes were repeated five times to adequately isolate the NPs from the RPP surface. The pre-experiment demonstrated that TOC could reach the maximum release after washing five times (Supplementary Figure 12). This solution was subjected to two filtration steps with PES filters to obtain the NP suspension.[7] The PES filters were washed with Milli-Q water three times before filtration experiments. Exactly 10 μm of PES was used in step 1 to remove the large particles in solution. Then the obtained filtrate I solution was subsequently filtered through 1 μm of PES twice to ensure that the filtered particles in filtrate II are on the nanometer scale (Figure 2). All experiments were performed in triplicate. In blank experiment, Milli-Q ultrapure water was filtered through the above-mentioned filtration steps. Results showed the TOC in blank filtrate II was only 0.23 mg/L (Supplementary Table 1), suggesting that the released substances from PES filters were negligible during filtration.

https://dx.doi.org/10.1021/acsnano.0c02878
ACS Nano XXXX, XXX, XXX−XXX

Characterization of the Released Nanoparticles and their Aggregates. The total organic carbon (TOC) of filtrate II was measured using a TOC analyzer (muti N/C 3100, Analytikjena, Germany). Dynamic light scattering (Marlvern Instruments, Ltd., Worcestershire, UK) was used as a preliminary technique for confirming the presence of organic matter in filtrate II.[7] The zeta potential of the released colloids was measured using the Zetasizer Nano with electrophoretic mobility analyses.

For the identification of the released nanoparticles, filtrate II was drop-casted on silicon wafer and subsequently air-dried for the conduct of RISE analysis on individual nanoparticles (Figure 2). In the preliminary experiment of standard nanosized PVC particles, a good image location and matching accuracy between SEM and Raman can be achieved through RISE analysis (Supplementary Figure 7). Interestingly, Raman spectral mapping (2 dimensions X, Y (2D)) in RISE can be used in screening nanoaggregates and describing the chemical distribution in a particle surface. Raman data were collected point by point in a 2D array consisting of an abundant of complete spectra. The point-by-point mapping consumed ~20 min for the scanning of 5 μm × 5 μm and 400 points (20 × 20) of the sample with an integration time of 2 s per point.

ASSOCIATED CONTENT

Supporting Information

The Supporting Information is available free of charge at https://pubs.acs.org/doi/10.1021/acsnano.0c02878.

FTIR, SEM, and Raman of RPP, Raman of $CaCO_3$ and standard PVC, SEM of RPP after washing, size distribution of particles in filtrate II, RPP, and standard PVC, SEM and Raman of S5, image location and matching for nano-PVC and RPP between SEM and Raman, time-dependent TOC of suspension during the washing experiment, and selected characteristics of RPP and the leachate (PDF)

AUTHOR INFORMATION

Corresponding Author

Yuping Qiu − *State Key Laboratory of Pollution Control and Resource Reuse, Ministry of Education Key Laboratory of Yangtze River Water Environment, Shanghai Institute of Pollution Control and Ecological Security, College of Environmental Science and Engineering, Tongji University, Shanghai 200092, China;* orcid.org/0000-0002-3803-1393; Phone: +86 02165983869; Email: ypqiu@tongji.edu.cn; Fax: +86 02165983869

Authors

Wen Zhang − *State Key Laboratory of Pollution Control and Resource Reuse, Ministry of Education Key Laboratory of Yangtze River Water Environment, Shanghai Institute of Pollution Control and Ecological Security, College of Environmental Science and Engineering, Tongji University, Shanghai 200092, China*

Zhiqiang Dong − *State Key Laboratory of Pollution Control and Resource Reuse, Ministry of Education Key Laboratory of Yangtze River Water Environment, Shanghai Institute of Pollution Control and Ecological Security, College of Environmental Science and Engineering, Tongji University, Shanghai 200092, China*

Ling Zhu − *State Key Laboratory of Pollution Control and Resource Reuse, Ministry of Education Key Laboratory of Yangtze River Water Environment, Shanghai Institute of Pollution Control and Ecological Security, College of Environmental Science and Engineering, Tongji University, Shanghai 200092, China*

Yuanzhang Hou − *State Key Laboratory of Pollution Control and Resource Reuse, Ministry of Education Key Laboratory of Yangtze River Water Environment, Shanghai Institute of Pollution Control and Ecological Security, College of Environmental Science and Engineering, Tongji University, Shanghai 200092, China*

Complete contact information is available at: https://pubs.acs.org/10.1021/acsnano.0c02878

Author Contributions

†W.Z. and Z.D. contributed equally to this work. The manuscript was written through contributions of all authors. All authors have given approval to the final version of the manuscript.

Notes

The authors declare no competing financial interest.

ACKNOWLEDGMENTS

This research was supported by the National Key Research and Development Program of China (2019YFC1805202) and the National Natural Science Foundation of China (21677108). We acknowledge the editor and the anonymous reviewers for their insightful suggestions and comments on our manuscript.

REFERENCES

(1) Hartmann, N. B.; Huffer, T.; Thompson, R. C.; Hassellov, M.; Verschoor, A. J.; Daugaard, A. E.; Rist, S.; Karlsson, K.; Brennholt, N.; Cole, M.; Herrling, M. P.; Hess, M. C.; Ivleva, N. P.; Lusher, A. L.; Wagner, M. Are We Speaking the Same Language? Recommendations for a Definition and Categorization Framework for Plastic Debris. *Environ. Sci. Technol.* **2019**, *53*, 1039−1047.

(2) Wagner, S.; Reemtsma, T. Things We Know and don't Know about Nanoplastic in the Environment. *Nat. Nanotechnol.* **2019**, *14*, 300−301.

(3) Ter Halle, A.; Jeanneau, L.; Martignac, M.; Jarde, E.; Pedrono, B.; Brach, L.; Gigault, J. Nanoplastic in the North Atlantic Subtropical Gyre. *Environ. Sci. Technol.* **2017**, *51*, 13689−13697.

(4) Dawson, A. L.; Kawaguchi, S.; King, C. K.; Townsend, K. A.; King, R.; Huston, W. M.; Bengtson Nash, S. M. Turning Microplastics into Nanoplastics through Digestive Fragmentation by Antarctic Krill. *Nat. Commun.* **2018**, *9*, 1−8.

(5) Magri, D.; Sanchez-Moreno, P.; Caputo, G.; Gatto, F.; Veronesi, M.; Bardi, G.; Catelani, T.; Guarnieri, D.; Athanassiou, A.; Pompa, P. P.; Fragouli, D. Laser Ablation as a Versatile Tool to Mimic Polyethylene Terephthalate Nanoplastic Pollutants: Characterization and Toxicology Assessment. *ACS Nano* **2018**, *12*, 7690−7700.

(6) Wang, T.; Wang, L.; Li, X.; Hu, X.; Han, Y.; Luo, Y.; Wang, Z.; Li, Q.; Aldalbahi, A.; Wang, L.; Song, S.; Fan, C.; Zhao, Y.; Wang, M.; Chen, N. Size-Dependent Regulation of Intracellular Trafficking of Polystyrene Nanoparticle-Based Drug-Delivery Systems. *ACS Appl. Mater. Interfaces* **2017**, *9*, 18619−18625.

(7) Hernandez, L. M.; Yousefi, N.; Tufenkji, N. Are There Nanoplastics in Your Personal Care Products? *Environ. Sci. Technol. Lett.* **2017**, *4*, 280−285.

(8) Koelmans, A. A. Proxies for Nanoplastic. *Nat. Nanotechnol.* **2019**, *14*, 307−308.

(9) Lambert, S.; Wagner, M. Characterisation of Nanoplastics during the Degradation of Polystyrene. *Chemosphere* **2016**, *145*, 265−268.

(10) Ekvall, M. T.; Lundqvist, M.; Kelpsiene, E.; Šileikis, E.; Gunnarsson, S. B.; Cedervall, T. Nanoplastics Formed during the Mechanical Breakdown of Daily-Use Polystyrene Products. *Nanoscale Adv.* **2019**, *1*, 1055−1061.

(11) González-Pleiter, M.; Tamayo-Belda, M.; Pulido-Reyes, G.; Amariei, G.; Leganés, F.; Rosal, R.; Fernández-Piñas, F. Secondary Nanoplastics Released from a Biodegradable Microplastic Severely

Impact Freshwater Environments. *Environ. Sci.: Nano* **2019**, *6*, 1382−1392.
(12) Hernandez, L. M.; Xu, E. G.; Larsson, H. C. E.; Tahara, R.; Maisuria, V. B.; Tufenkji, N. Plastic Teabags Release Billions of Microparticles and Nanoparticles into Tea. *Environ. Sci. Technol.* **2019**, *53*, 12300−12310.
(13) Lehner, R.; Weder, C.; Petri-Fink, A.; Rothen-Rutishauser, B. Emergence of Nanoplastic in the Environment and Possible Impact on Human Health. *Environ. Sci. Technol.* **2019**, *53*, 1748−1765.
(14) Strungaru, S.-A.; Jijie, R.; Nicoara, M.; Plavan, G.; Faggio, C. Micro-(Nano) Plastics in Freshwater Ecosystems: Abundance, Toxicological Impact and Quantification Methodology. *TrAC, Trends Anal. Chem.* **2019**, *110*, 116−128.
(15) Mattsson, K.; Johnson, E. V.; Malmendal, A.; Linse, S.; Hansson, L.-A.; Cedervall, T. Brain Damage and Behavioural Disorders in Fish Induced by Plastic Nanoparticles Delivered through the Food Chain. *Sci. Rep.* **2017**, *7*, 1−7.
(16) Zhang, Y.; Wang, X.; Shan, J.; Zhao, J.; Zhang, W.; Liu, L.; Wu, F. Hyperspectral Imaging-Based Method for Rapid Detection of Microplastics in the Intestinal Tracts of Fish. *Environ. Sci. Technol.* **2019**, *53*, 5151−5158.
(17) He, H.-J.; Sun, D.-W. Hyperspectral Imaging Technology for Rapid Detection of Various Microbial Contaminants in Agricultural and Food Products. *Trends Food Sci. Technol.* **2015**, *46*, 99−109.
(18) Araujo, C. F.; Nolasco, M. M.; Ribeiro, A. M. P.; Ribeiro-Claro, P. J. A. Identification of Microplastics Using Raman Spectroscopy: Latest Developments and Future Prospects. *Water Res.* **2018**, *142*, 426−440.
(19) Cabernard, L.; Roscher, L.; Lorenz, C.; Gerdts, G.; Primpke, S. Comparison of Raman and Fourier Transform Infrared Spectroscopy for the Quantification of Microplastics in the Aquatic Environment. *Environ. Sci. Technol.* **2018**, *52*, 13279−13288.
(20) Schmidt, U.; Liu, W.; Yang, J.; Dieing, T.; Weishaupt, K. The Power of Confocal Raman-AFM and Raman-SEM (RISE) Imaging in Polymer Research. *Microsc. Microanal.* **2015**, *21*, 2189−2190.
(21) Schmidt, U.; Zimmermann, H.; Freitag, S.; Dieing, T. RISE - Raman SEM Imaging of Single Layer and Twisted Bilayer Graphene. *Microsc. Microanal.* **2017**, *23*, 1748−1749.
(22) Wille, G.; Schmidt, U.; Hollricher, O. RISE: Correlative Confocal Raman and Scanning Electron Microscopy. In *Confocal Raman Microscopy*; Toporski, J., Dieing, T., Hollricher, O., Eds.; Springer Series in Surface Sciences, Vol. 66; Springer: Cham, Switzerland, 2018; pp 559−580.
(23) Suresh, S. S.; Mohanty, S.; Nayak, S. K. Composition Analysis and Characterization of Waste Polyvinyl Chloride (PVC) Recovered from Data Cables. *Waste Manage.* **2017**, *60*, 100−111.
(24) Zhou, Y.; Yang, N.; Hu, S. Industrial Metabolism of PVC in China: A Dynamic Material Flow Analysis. *Resour. Conser. Recy.* **2013**, *73*, 33−40.
(25) Geyer, R.; Jambeck, J. R.; Law, K. L. Production, Use, and Fate of All Plastics Ever Made. *Sci. Adv.* **2017**, *3*, No. e1700782.
(26) Janajreh, I.; Alshrah, M.; Zamzam, S. Mechanical Recycling of PVC Plastic Waste Streams from Cable Industry: A Case Study. *Sustain. Cities Soc.* **2015**, *18*, 13−20.
(27) Lenz, R.; Enders, K.; Stedmon, C. A.; Mackenzie, D. M. A.; Nielsen, T. G. A Critical Assessment of Visual Identification of Marine Microplastic Using Raman Spectroscopy for Analysis Improvement. *Mar. Pollut. Bull.* **2015**, *100*, 82−91.
(28) Uddin, A. J.; Araki, J.; Gotoh, Y. Characterization of the Poly(Vinyl Alcohol)/Cellulose Whisker Gel Spun Fibers. *Composites, Part A* **2011**, *42*, 741−747.
(29) Imhof, H. K.; Laforsch, C.; Wiesheu, A. C.; Schmid, J.; Anger, P. M.; Niessner, R.; Ivleva, N. P. Pigments and Plastic in Limnetic Ecosystems: A Qualitative and Quantitative Study on Microparticles of Different Size Classes. *Water Res.* **2016**, *98*, 64−74.
(30) Ossmann, B. E.; Sarau, G.; Holtmannspotter, H.; Pischetsrieder, M.; Christiansen, S. H.; Dicke, W. Small-Sized Microplastics and Pigmented Particles in Bottled Mineral Water. *Water Res.* **2018**, *141*, 307−316.
(31) Romera-Castillo, C.; Pinto, M.; Langer, T. M.; Alvarez-Salgado, X. A.; Herndl, G. J. Dissolved Organic Carbon Leaching from Plastics Stimulates Microbial Activity in the Ocean. *Nat. Commun.* **2018**, *9*, 1−7.
(32) Gigault, J.; Halle, A. T.; Baudrimont, M.; Pascal, P. Y.; Gauffre, F.; Phi, T. L.; El Hadri, H.; Grassl, B.; Reynaud, S. Current Opinion: What Is a Nanoplastic? *Environ. Pollut.* **2018**, *235*, 1030−1034.
(33) Guermazi, N.; Haddar, N.; Elleuch, K.; Ayedi, H. F. Effect of Filler Addition and Weathering Conditions on the Performance of PVC/$CaCO_3$ Composites. *Polym. Compos.* **2016**, *37*, 2171−2183.
(34) Schwaferts, C.; Niessner, R.; Elsner, M.; Ivleva, N. P. Methods for the Analysis of Submicrometer- and Nanoplastic Particles in the Environment. *TrAC, Trends Anal. Chem.* **2019**, *112*, 52−65.
(35) Nguyen, B.; Claveau-Mallet, D.; Hernandez, L. M.; Xu, E. G.; Farner, J. M.; Tufenkji, N. Separation and Analysis of Microplastics and Nanoplastics in Complex Environmental Samples. *Acc. Chem. Res.* **2019**, *52*, 858−866.
(36) Gillibert, R.; Balakrishnan, G.; Deshoules, Q.; Tardivel, M.; Magazzù, A.; Donato, M. G.; Marago, O. M.; de La Chapelle, M. L.; Colas, F.; Lagarde, F. Raman Tweezers for Small Microplastics and Nanoplastics Identification in Seawater. *Environ. Sci. Technol.* **2019**, *53*, 9003−9013.
(37) Gu, F.; Guo, J.; Zhang, W.; Summers, P. A.; Hall, P. From Waste Plastics to Industrial Raw Materials: A Life Cycle Assessment of Mechanical Plastic Recycling Practice Based on a Real-World Case Study. *Sci. Total Environ.* **2017**, *601*, 1192−1207.
(38) Garcia, J. M.; Robertson, M. L. The Future of Plastics Recycling. *Science* **2017**, *358*, 870−872.
(39) Enfrin, M. Release of Hazardous Nanoplastic Contaminants Due to Microplastics Fragmentation under Shear Stress Forces. *J. Hazard. Mater.* **2020**, *384*, 121393.
(40) Yang, R. D.; Tripathy, S.; Li, Y.; Sue, H. J. Photoluminescence and Micro-Raman Scattering in ZnO Nanoparticles: The Influence of Acetate Adsorption. *Chem. Phys. Lett.* **2005**, *411*, 150−154.
(41) Yang, R. D.; Tripathy, S.; Tay, F. E.; Gan, L.; Chua, S. Photoluminescence and Micro-Raman Scattering in Mn-Doped ZnS Nanocrystalline Semiconductors. *J. Vac. Sci. Technol., B: Microelectron. Process. Phenom.* **2003**, *21*, 984−988.
(42) Yang, C.; Li, S. Size-Dependent Raman Red Shifts of Semiconductor Nanocrystals. *J. Phys. Chem. B* **2008**, *112*, 14193−14197.
(43) Galloway, T. S.; Cole, M.; Lewis, C. Interactions of Microplastic Debris throughout the Marine Ecosystem. *Nat. Ecol. Evol.* **2017**, *1*, 1−8.

https://dx.doi.org/10.1021/acsnano.0c02878
ACS Nano XXXX, XXX, XXX−XXX